Geohazard Mechanics 4 (2026) 55–66

Contents lists available at ScienceDirect

Geohazard Mechanics

journal homepage: www.keaipublishing.com/en/journals/geohazard-mechanics

Landslide susceptibility assessment of Western Ghats of Karnataka region in India: A case study of Ankola landslide

Malay Pramanik*, Amarnath Hegde

Department of Civil & Infrastructure Engineering, Indian Institute of Technology Dharwad, Dharwad, 580011, India

ARTICLE INFO

Keywords:
Landslide
Susceptibility
Western ghats
Geographic information system
Hybrid analytical approach

ABSTRACT

Recurring and frequent landslides in the Western Ghats of India pose major socio-economic challenges by interrupting the infrastructure development and daily life. The present study evaluates the landslide susceptibility of the region using a hybrid approach. Data from various sources including satellite images, past landslide records, geological, topographical and hydrological datasets was utilized to develop landslide inventory and the causative factors of the study area. The adopted hybrid approach integrates the analytic hierarchy process (AHP) and relative frequency ratio. The model demonstrated excellent discriminatory ability with an area under the ROC curve (AUC) of 0.902. The Uttara Kannada district has been identified as most susceptible to landslide in Karnataka. Further, the recent Ankola landslide in the highly susceptible Uttara Kannada was taken for a detailed case study. The field observations, geotechnical characterization, and rainfall details of the landslide site suggest that the anthropogenic activity and heavy rainfall were the reasons for triggering the landslide. The landslide event was back-analysed using pore water pressure factor (R_u) to simulate pore-water pressure development during rainfall. The R_u factor of 0.4 was identified as critical threshold for initiating slope failures, providing a quantitative basis for early warning systems for the region. The susceptibility model and the R_u factor threshold found in the study offer essential information for the enhancement of risk mitigation efforts in the Western Ghats.

1. Introduction

Landslide is the most significant geohazards in mountainous areas which affects infrastructure, ecosystems, and human beings. The frequency and severity of fatal landslides have escalated in South Asian countries like India, Nepal, and China. This escalation is mostly attributable to rapid urbanization, deforestation, poorly planned infrastructure, and climate change-induced alterations in rainfall patterns [1]. To mitigate the socio-economic impacts of these disasters, it is essential to implement efficient landslide risk reduction strategies [2]. Landslide susceptibility mapping is the foundation of the mitigation strategies, as it delineates areas prone to landslides. Susceptibility mapping entails analysing the spatial relationship between historical occurrences and their causative factors [3–5]. The emergence of advanced remote sensing and geographic information system (GIS) techniques has transformed landslide susceptibility assessments from rudimentary qualitative methods to sophisticated quantitative approaches [3,6]. Despite these advancements, issues in model generalization, data quality, and region-specific validation remained. These limitations underscore the necessity for further methodological enhancement [7].

Qualitative methods are among the earliest tools used for hazard zonation. These methods are primarily based on expert opinion and field observations, which imparts high level of subjectivity and inability to replicability [8,9]. An attempt was made to eliminate these drawbacks by introducing semi-quantitative techniques such as the analytic hierarchy process (AHP) and weights-of-evidence. These methods employ systematic frameworks that assign weights to contributing factors [4,10]. However, these methods continue to rely on subjective judgments and fail to reflect the probabilistic nature of landslide occurrence. Through data-driven analysis, statistical and machine learning algorithms based quantitative models demonstrated a significant advancement [11–17]. These models demand extensive high-quality datasets, which can be difficult to obtain for many regions. These constraints underscore the necessity of hybrid models that can eliminate these issues [18]. In regions with complex terrain and limited data availability, integrated frameworks can provide a balanced solution for landslide susceptibility mapping [19,20]. While the development of landslide susceptibility map is essential, their practical value depends on rigorous

* Corresponding author.
E-mail address: ce23dp005@iitdh.ac.in (M. Pramanik).
Peer review under the responsibility of Liaoning University.

https://doi.org/10.1016/j.ghm.2026.01.003
Received 7 May 2025; Received in revised form 29 August 2025; Accepted 7 January 2026
Available online 12 January 2026

validation [21]. Empirically derived models must be corroborated through field investigations to ensure that predicted high-susceptible zones align with ground realities.

The Western Ghats region is recognized as a biodiversity hotspot and experiencing rapid change of landuse. This region has recently witnessed an alarming rise in fatal landslides [22]. In 2024 alone, the Western Ghats region has experienced more than 40 landslides. The disastrous Wayanad landslides caused the loss of over 250 lives and the destruction of multiple villages, while another fatal landslide in Ankola underlined the region's increasing susceptibility [23]. These incidents have raised apprehension and elicited significant governmental response. The Government of India has initiated the National Landslide Risk Mitigation Project (NLRMP) focusing on 15 landslide-prone states. The project includes four states in the Western Ghats region such as Karnataka, Kerala, Maharashtra, and Tamil Nadu [24]. The initiative fosters the advancement of mitigating infrastructure, real-time monitoring, and preparedness. However, the absence of reliable susceptibility maps remains a major obstacle. Addressing this shortcoming underscores the strategic importance of the current study in enabling the planning of mitigation measures in the Western Ghats.

Few studies have investigated landslide susceptibility in the Western Ghats using different techniques. Sajinkumar and Anbazhagan applied GIS-based heuristic methods to integrate multi-temporal landslide inventories with geomorphological and hydrological factors [25]. Vijith et al. utilized a weights-of-evidence approach to map shallow landslide initiation zones by combining multiple terrain parameters [26]. Feby et al. adopted logistic regression and statistical models to evaluate susceptibility in selected parts of the region [27,28]. These studies provided valuable insights but exhibited certain limitations. Most studies relied on subjective factor weighting or used single statistical models without validating their models against recent major landslide events. The present study addresses these gaps by utilizing a hybrid framework. This hybrid approach combines expert-based factor prioritization with objective statistical correlation. The study aims to evaluate landslide susceptibility in the Western Ghats region of India. A case study was also incorporated to demonstrate the relevance and practical applicability of the susceptibility map. This integrated framework improves the accuracy and reinforces the reliability of the landslide susceptibility model.

2. Study area

The current study focuses on the Western Ghats region in the Karnataka state of India, covering approximately 45,000 km^2 in southwestern India, span from 11.5°N to 16.3°N latitude and from 74°E to 76.7°E longitude. Fig. 1 shows the study area in India along with the locations of past landslides. The study area comprises seven districts of Karnataka state, including Uttara Kannada, Shivamogga, Udupi, Chikkamagaluru, Hassan, Kodagu, and Dakshina Kannada. The past landslide data was obtained from the Bhukosh portal of the Geological Survey of India (GSI). It contains a total 1270 landslide events across the Western Ghats of Karnataka from 1998 to 2020. These events were particularly prevalent during the monsoon period when intense and prolonged rainfall occurred in this region [29].

2.1. Landslide causative factors

Landslides are caused by of a combination of geological, topographical, hydrological, and anthropogenic factors [30]. These factors are diverse and often site-specific, reflecting the unique conditions of an area [31]. Landslide causative factors were carefully selected from reliable authoritative sources and resampled to widely accepted effective resolution of 30 m [32–34]. The data on past landslides and causative factors of landslides in the study area were compiled from several sources, as shown in Table 1. The past landslide data from GSI was used to create a landslide inventory for the study area. The inventory was divided into two subsets: 70 % of the dataset was used for training the model, while the remaining 30 % was reserved for testing. This division ensures that the model's performance can be evaluated on an independent dataset, thereby validating its predictive accuracy of the susceptibility model [35,36].

The raw data of all the causative factors was procured and carefully pre-processed as follows. All datasets were initially cropped to align with the study area's boundary. Each dataset was converted into a raster map to enable comprehensive spatial analysis within a GIS framework. For this study, ArcGIS Pro 2.9.0 was used. The raster maps were resampled to 30 m resolution using the bilinear interpolation technique to achieve a consistent spatial resolution across all the data sets. The 30 m × 30 m resolution was chosen to balance spatial detail and computational efficiency. This resolution is widely adopted for terrain-

Table 1
Data and its sources.

Data	Source	Resolution/scale
Past landslides	Bhukosh, Geological Survey of India	
Soil	Food & Agriculture Organisation (FAO), USA	1:5 million
Topography	National Remote Sensing Centre, India	30 m
Rainfall	Climatic Research Unit (CRU), UK	50 m
Lineaments	Bhukosh, Geological Survey of India	
Road network	Bhukosh, Geological Survey of India	
Landcover	Sentinel-2 satellite image	10 m

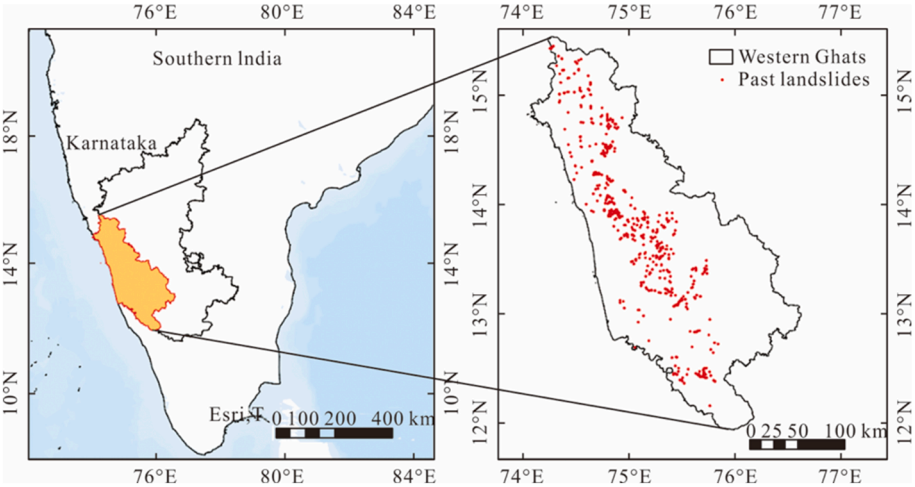

Fig. 1. Study area (Western Ghats region in Karnataka) and past landslide locations.

driven landslide susceptibility analysis as it corresponds to the resolution of commonly used DEMs such as the shuttle radar topography mission (SRTM) [37,38]. Following resampling, each dataset was systematically reclassified into multiple subclasses to facilitate ease of analysis. For instance, mean annual rainfall was reclassified into very low, low, moderate, high, very high, and extreme.

Fig. 2a–j shows the maps of landslide causative factors in the study area, which include topographical, geological, hydrological, and anthropogenic factors. Topographical parameters include slope gradient, elevation, slope aspect, and curvature. These datasets were

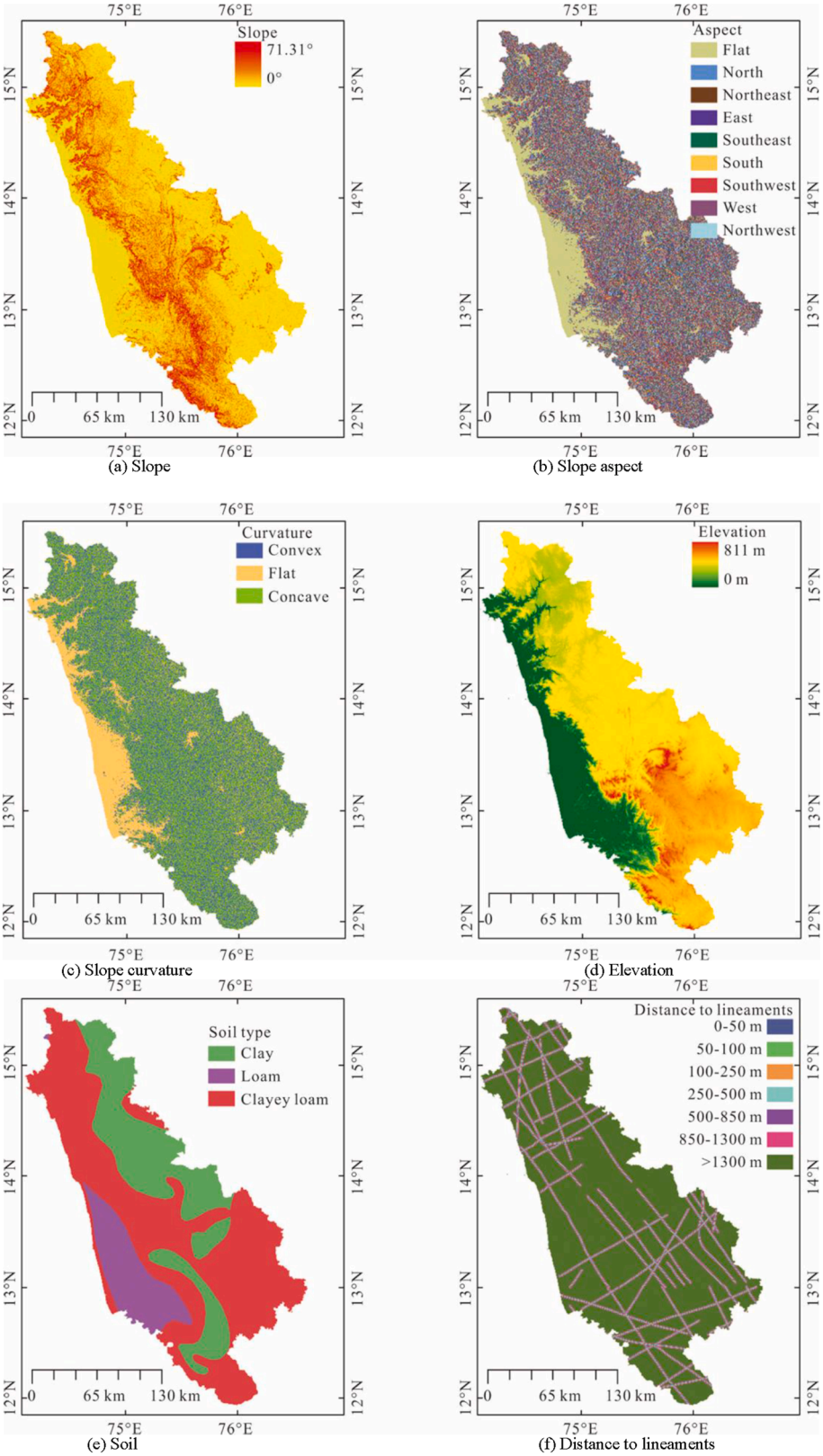

Fig. 2. Landslide causative factors.

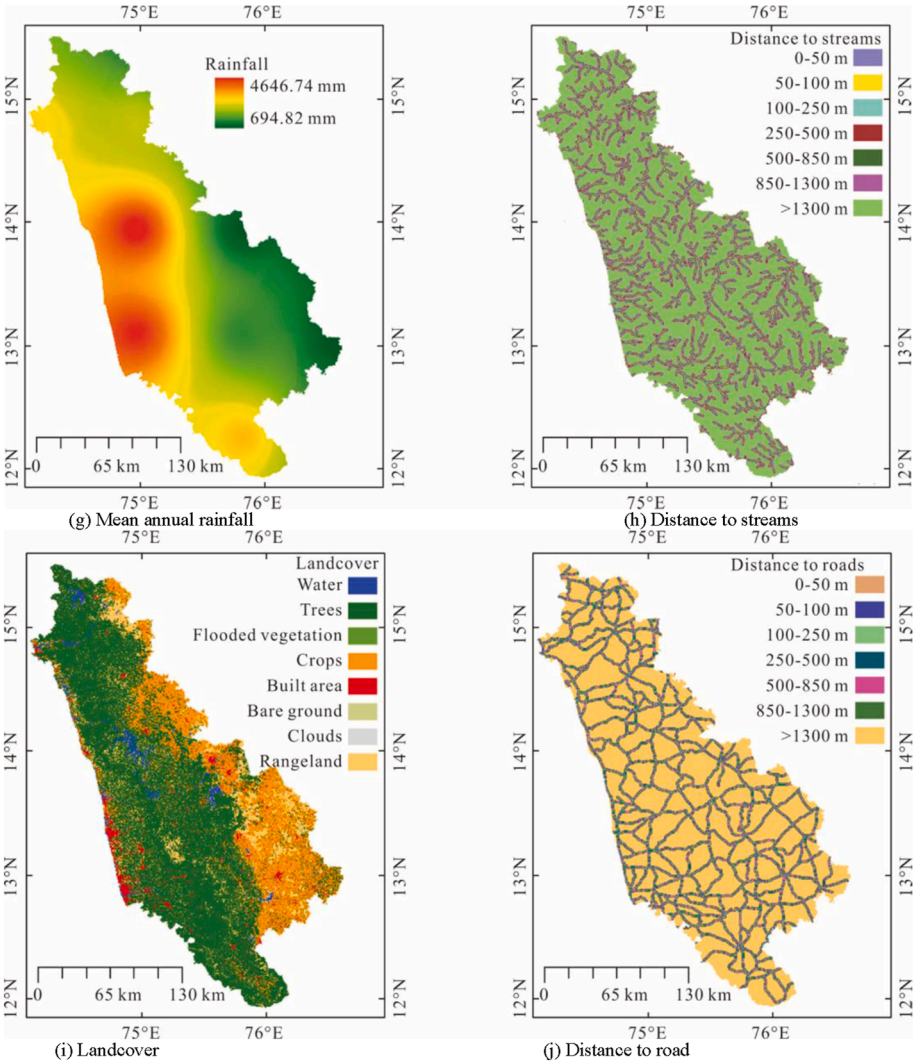

Fig. 2. (*continued*).

obtained from a digital elevation model (DEM), which was generated from Cartosat-1 satellite images. The stream network of the study area was also generated from the same DEM. The region is characterized by varying slope gradient ranges from flat terrain to 70°, and elevations ranging from 0 to 1811 m. The soil types and lineaments were considered key geological factors for the study. The region basically has three types of soil: clay, clayey loam, and loam. The study area mostly comprised of clay and clayey loam covering an area of 28 % and 59 %, respectively. The hydrological factors include the mean annual rainfall, which was obtained from past 30 years records. The mean annual rainfall in the region ranges from 695 to 4647 mm. Notably, 70 % of the area receives more than 2000 mm rainfall annually. The anthropogenic factors such as road construction, slope cutting, and vegetation were considered implicitly through the landcover and road network data [39–41]. Collectively, these datasets facilitate a comprehensive assessment of the susceptibility to landslides.

2.2. Susceptibility map of Western Ghats region in Karnataka

Choosing a landslide susceptibility assessment method is crucial for accurately capturing the complex interplay of causative factors that influence slope stability in the Western Ghats. This study adopted a hybrid approach that combines the analytical hierarchy process (AHP) and relative frequency ratio (RFR). The integration of the AHP and RFR method provides a framework that effectively addresses the inherent limitations of each individual approach. AHP is frequently criticized for its subjectivity and lack of empirical justification [42]. However, the subjectivity was minimised with acceptable threshold (<10 %) of consistency ratio (CR) of the pairwise comparison matrix (PCM). The PCM with CR is presented in Table 2. Conversely, RFR is a data-driven methodology that quantifies the relationship between historical events and conditioning factors, providing statistical precision [43]. However, it is heavily dependent on the quality and availability of past data, which poses a potential risk of overfitting. The hybrid approach ensures that the inherent subjectivity of AHP is balanced by the statistical precision of RFR, while RFR benefits from the structured prioritization of causative factors offered by the AHP [44]. The landslide susceptibility index (LSI) for the study area is computed using Eq. (1) [45].

$$LSI = \sum FR_j \times W_j^f \quad (1)$$

where FR_j and W_j^f are the frequency ratio and weight of the jth causative factor, respectively. The weight of causative factors $\left(W_j^f\right)$ was calculated using the AHP. This process involves the construction of a pairwise comparison matrix. Then the matrix is used to calculate weights, which reflects the relative influence of each factor. The frequency ratios (FR_j) were calculated using the RFR method, by dividing the density of landslides within each factor by the overall landslide density in the study area. The computation follows Eq. (2) [45].

Table 2
Class-wise weighted factor evaluated using AHP.

Factor	Class	Pair-wise comparison matrix									Weighted factor (WF)
		(1)	(2)	(3)	(4)	(5)	(6)	(7)	(8)	(9)	
Rainfall	(1) >4000 mm	1	3	7	8	5	6				0.425
	(2) 3500–4000 mm	1/3	1	3	7	8	5				0.249
	(3) 3000–3500 mm	1/7	1/3	1	3	7	8				0.156
	(4) 2500–3000 mm	1/8	1/7	1/3	1	3	7				0.088
	(5) 2000–2500 mm	1/5	1/8	1/7	1/3	1	3				0.050
	(6) <2000 mm	1/6	1/5	1/8	1/7	1/3	1				0.032
		Consistency ratio = 0.086									
Soil	(1) Clay loam	1	4	7							0.688
	(2) Clay	1/4	1	4							0.234
	(3) Loam	1/7	1/4	1							0.078
		Consistency ratio = 0.074									
Slope	(1) >35°	1	3	5	7	9	9				0.452
	(2) 28°–35°	1/3	1	3	5	7	9				0.256
	(3) 21°–28°	1/5	1/3	1	3	5	7				0.144
	(4) 14°–21°	1/7	1/5	1/3	1	3	5				0.080
	(5) 7°–14°	1/9	1/7	1/5	1/3	1	3				0.043
	(6) <7°	1/9	1/9	1/7	1/5	1/3	1				0.025
		Consistency ratio = 0.075									
Landcover	(1) Trees	1	1	2	3	5	7	7	9		0.300
	(2) Rangeland	1	1	1	2	3	5	7	7		0.228
	(3) Built area	1/2	1	1	1	2	3	5	7		0.166
	(4) Water	1/3	1/2	1	1	1	2	3	5		0.114
	(5) Crops	1/5	1/3	1/2	1	1	1	2	3		0.076
	(6) Flooded vegetation	1/7	1/5	1/3	1/2	1	1	1	2		0.052
	(7) Bare grounds	1/7	1/7	1/5	1/3	1/2	1	1	1		0.037
	(8) Clouds	1/9	1/7	1/7	1/5	1/3	1/2	1	1		0.028
		Consistency ratio = 0.021									
Curvature	(1) Concave	1	3	4							0.608
	(2) Convex	1/3	1	3							0.272
	(3) Flat	1/4	1/3	1							0.120
		Consistency ratio = 0.071									
Elevation	(1) 227–490 m	1	3	5	7	9	9				0.452
	(2) >1022 m	1/3	1	3	5	7	9				0.256
	(3) 490–653 m	1/5	1/3	1	3	5	7				0.144
	(4) 816–1022 m	1/7	1/5	1/3	1	3	5				0.080
	(5) 653–816 m	1/9	1/7	1/5	1/3	1	3				0.043
	(6) <227 m	1/9	1/9	1/7	1/5	1/3	1				0.025
		Consistency ratio = 0.075									
Distance to road	(1) <50 m	1	2	4	6	8	9	9			0.419
	(2) 50–100 m	1/2	1	2	4	6	8	9			0.256
	(3) 100–250 m	1/4	1/2	1	2	4	6	8			0.147
	(4) 250–500 m	1/6	1/4	1/2	1	2	4	6			0.082
	(5) 500–750 m	1/8	1/6	1/4	1/2	1	2	4			0.046
	(6) 750–1000 m	1/9	1/8	1/6	1/4	1/2	1	2			0.029
	(7) >1000 m	1/9	1/9	1/8	1/6	1/4	1/2	1			0.022
		Consistency ratio = 0.041									
Distance to stream	(1) <50 m	1	2	4	6	8	9	9			0.419
	(2) 50–100 m	1/2	1	2	4	6	8	9			0.256
	(3) 100–250 m	1/4	1/2	1	2	4	6	8			0.147
	(4) 250–500 m	1/6	1/4	1/2	1	2	4	6			0.082
	(5) 500–750 m	1/8	1/6	1/4	1/2	1	2	4			0.046
	(6) 750–1000 m	1/9	1/8	1/6	1/4	1/2	1	2			0.029
	(7) >1000 m	1/9	1/9	1/8	1/6	1/4	1/2	1			0.022
		Consistency ratio = 0.041									
Distance to lineaments	(1) <50 m	1	2	4	6	8	9	9			0.419
	(2) 50–100 m	1/2	1	2	4	6	8	9			0.256
	(3) 100–250 m	1/4	1/2	1	2	4	6	8			0.147
	(4) 250–500 m	1/6	1/4	1/2	1	2	4	6			0.082
	(5) 500–750 m	1/8	1/6	1/4	1/2	1	2	4			0.046
	(6) 750–1000 m	1/9	1/8	1/6	1/4	1/2	1	2			0.029
	(7) >1000 m	1/9	1/9	1/8	1/6	1/4	1/2	1			0.022
		Consistency ratio = 0.041									
Slope aspect	(1) West	1	2	3	4	5	6	8	9	9	0.305
	(2) East	1/2	1	2	3	4	5	7	8	9	0.219
	(3) Southwest	1/3	1/2	1	2	3	4	6	7	8	0.156
	(4) North	1/4	1/3	1/2	1	2	3	5	6	7	0.111
	(5) Northeast	1/5	1/4	1/3	1/2	1	2	4	5	6	0.080
	(6) Northwest	1/6	1/5	1/4	1/3	1/2	1	3	4	5	0.058
	(7) Southeast	1/8	1/7	1/6	1/5	1/4	1/3	1	2	3	0.031
	(8) South	1/9	1/8	1/7	1/6	1/5	1/4	1/2	1	2	0.022
	(9) Flat	1/9	1/9	1/8	1/7	1/6	1/5	1/3	1/2	1	0.017
		Consistency ratio = 0.043									

$$FR_j = \frac{L_j/L_{total}}{A_j/A_{total}} \quad (2)$$

where L_j is the number of landslides occurred in areas with factor j; L_{total} is the total number of landslides; A_j is the area of factor j; and A_{total} is the total study area.

Table 3 outlines the classification and weightage of various causative factors influencing landslide susceptibility in the study area. Each factor plays a unique role in determining landslide susceptibility. The areas receiving a mean annual rainfall of 3000–3500 mm and 2500–3000 mm have the highest weights (0.473 and 0.271, respectively), underscoring the influence of intense rainfall in triggering landslides. Among the three types of soil, clay loam soils exhibit the highest weight (0.738), indicating a high susceptibility due to their tendency to retain water and reduce slope stability. Slope steepness is also crucial, with slopes greater than 35° showing the highest weight (0.546), as steeper slopes are inherently more prone to failure under gravitational stress. Landcover analysis reveals that tree-covered areas have the highest weight (0.652), while built-up areas and rangelands contribute to increased susceptibility with weights of 0.125 and 0.204, respectively. The curvature of slopes also affects stability, with concave slopes accumulating more water and having the highest weight (0.726). Elevation between 227 and 490 m is associated with the greatest susceptibility weight (0.536). Proximity to roads and streams further amplifies landslide susceptibility, as areas within 50 m of roads and streams are highly weighted (0.469 and 0.495, respectively). Lineaments, representing geological weaknesses such as faults and fractures, have the highest weight (0.588) for areas within 50 m, reflecting the vulnerability of such zones to landslides. Lastly, the slope aspect influences susceptibility, with west-facing slopes receiving the highest weight (0.402), possibly due to prevailing weather patterns contributing to erosion and slope instability.

Fig. 3 shows the influence factor of each causative factors on landslide occurrences, based on the susceptibility model. The analysis reveals that slope gradient and mean annual rainfall are the critical factors

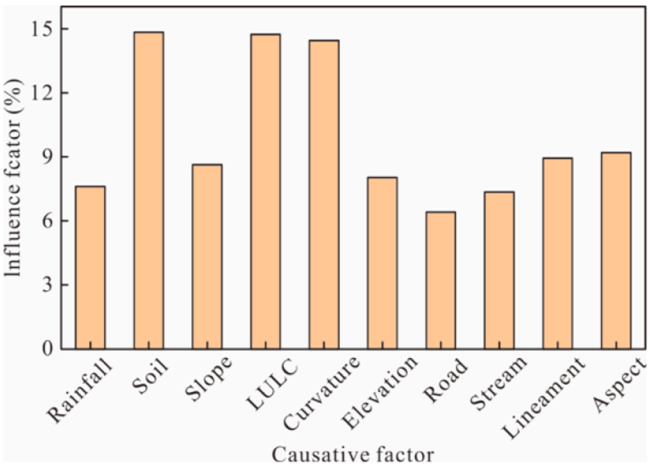

Fig. 3. Influence of causative factors on landslide occurrence.

with influence factor of 26.17 % and 16.02 %, respectively. It emphasizes the role of steep topography and heavy monsoon precipitation in triggering landslides. Soil type (18 %) and land cover (16 %) also have significant impacts, highlighting the importance of soil stability and vegetation cover in slope protection. Slope curvature (10 %) moderately affects landslide susceptibility, influencing slope water accumulation. Factors such as distance to lineaments (5 %) and distance to streams (3 %) have lower impacts, while elevation (2 %), distance to roads (1 %), and slope aspect (0.5 %) show minimal influence. This varied influence of the causative factors underscores the need to prioritize factors like slope gradient, rainfall, soil type and landcover in landslide susceptibility assessment.

The landslide susceptibility map of the study area is presented in Fig. 4a. It shows that a substantial portion of the Western Ghats in Karnataka is susceptible to landslides. Fig. 4b and c shows distribution of

Table 3
Weightage of causative factors.

Factor	Class	Class weightage	Factor	Class	Class weightage
Rainfall	<2000 mm	0.000	Elevation	<227 m	0.008
	2000–2500 mm	0.020		227–490 m	0.536
	2500–3000 mm	0.271		490–653 m	0.134
	3000–3500 mm	0.473		653–816 m	0.019
	3500–4000 mm	0.072		816–1022 m	0.050
	>4000 mm	0.165		>1022 m	0.253
Soil	Clay	0.250	Curvature	Concave	0.726
	Loam	0.011		Flat	0.012
	Clay loam	0.738		Convex	0.262
Slope	<7°	0.000	Distance to road	<50 m	0.469
	7°–14°	0.015		50–100 m	0.245
	14°–21°	0.041		100–250 m	0.159
	21°–28°	0.128		250–500 m	0.075
	28°–35°	0.270		500–750 m	0.034
	>35°	0.546		750–1000 m	0.013
				>1000 m	0.004
Distance to stream	<50 m	0.495	Distance to lineaments	<50 m	0.588
	50–100 m	0.314		50–100 m	0.222
	100–250 m	0.095		100–250 m	0.075
	250–500 m	0.043		250–500 m	0.075
	500–750 m	0.026		500–750 m	0.019
	750–1000 m	0.012		750–1000 m	0.013
	>1000 m	0.015		>1000 m	0.008
Slope aspect	Flat	0.000	Landcover	Water	0.016
	North	0.010		Trees	0.652
	Northeast	0.078		Flooded vegetation	0.000
	East	0.246		Crops	0.003
	Southeast	0.025		Built area	0.125
	South	0.017		Bare grounds	0.000
	Southwest	0.167		Clouds	0.000
	West	0.402		Rangeland	0.204
	Northwest	0.055			

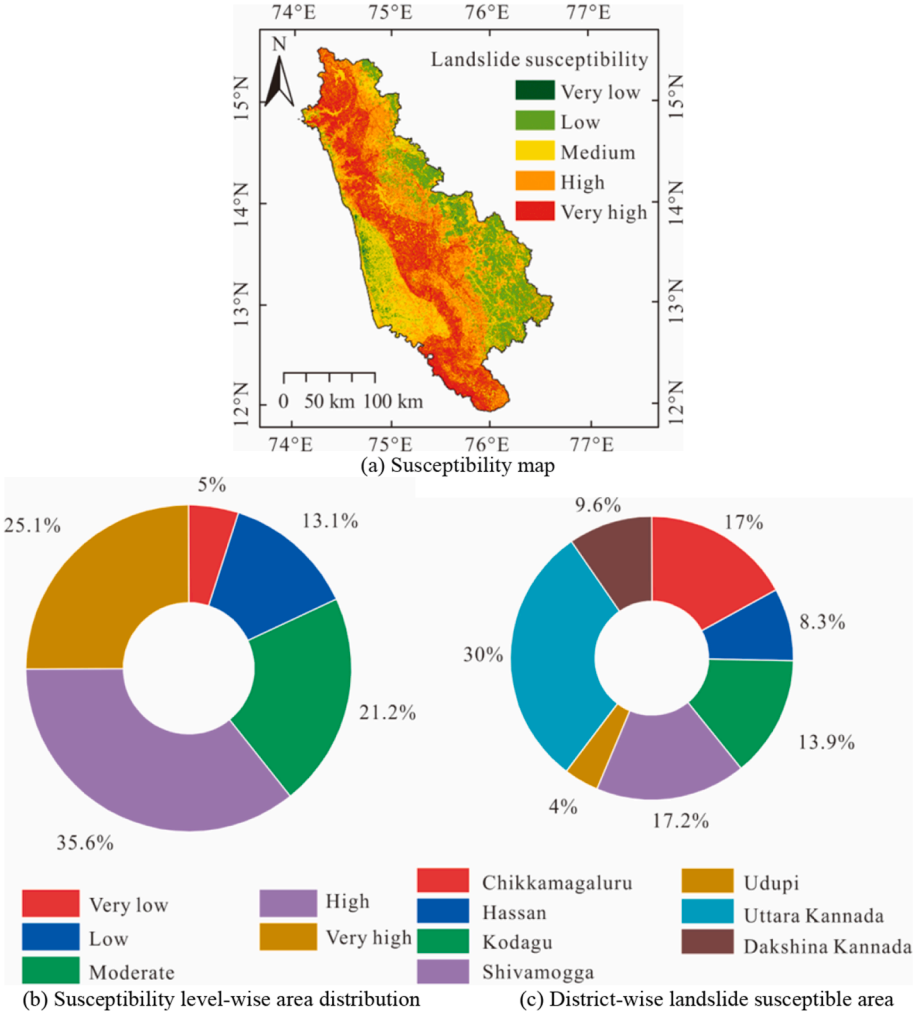

Fig. 4. Landslide susceptibility map and area distribution.

landslide susceptible areas in the seven districts of Karnataka state. Approximately 35.6 % and 25.1 % of the study area fall within the high and very high susceptibility zones, respectively. The medium susceptibility class covers 21.24 % area of the region. Meanwhile, low and very low susceptibility zones account for only 18.06 % of the study area. The study identifies Uttara Kannada district having the highest proportion of areas susceptible to landslides, encompassing about 30 % of the total susceptible area. Shivamogga and Chikkamagaluru districts follow with 17.18 % and 17 % respectively of the susceptible areas. Kodagu, Dakshina Kannada, and Hassan districts also show considerable susceptibility, with 13.88 %, 9.63 %, and 8.26 %, respectively. Udupi district has the least susceptibility, comprising only 4 % of the area prone to landslides.

This study uses the receiver operating curve (ROC) method to validate the hybrid landslide susceptibility model. Fig. 5 shows the ROC curve for the landslide susceptibility model. The steep initial rise reflects a high true positive rate with minimal false positives, making it well-suited for practical applications. The flat curve toward the upper side is indicating the potential for some false positives. However, the high AUC value of 0.902 validates reliability of the model. The AUC value obtained in this study is comparable with machine learning models reported by several researchers [16,41], supporting the robustness of the hybrid approach.

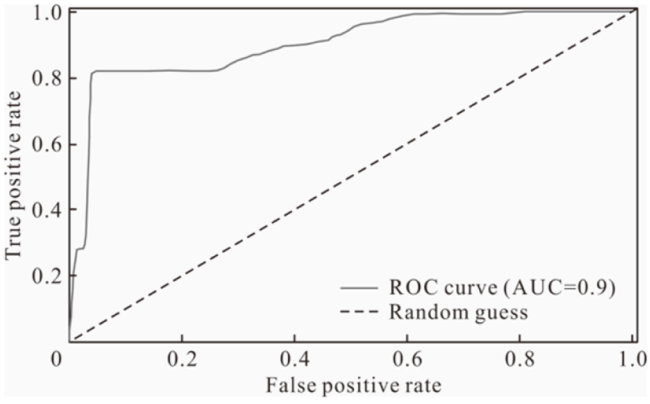

Fig. 5. ROC curve for the susceptibility model.

3. A case study of Ankola landslide

The present study investigates a landslide event which occurred in Ankola on July 16, 2024. The landslide located in the highly susceptible Uttara Kannada district of Karnataka state at 14.605°N, 74.371°E. Fig. 6a displays an image from Google Earth showing the landslide site with a red circle. The landslide site is adjacent to the National Highway 66, with the River Gangavali flowing nearby. Fig. 6b locates the landslide within the Uttara Kannada district on a map of Karnataka state. The area experienced substantial rainfall on the day of the landslide, recording 195 mm, with a total of 324 mm in three days of antecedent

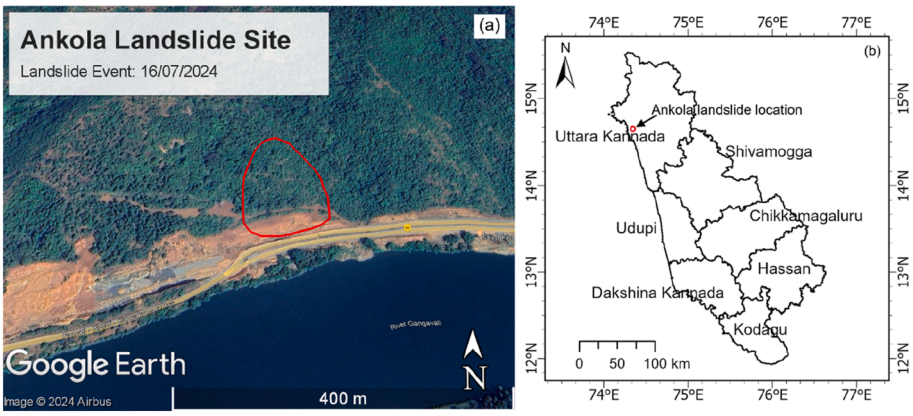

Fig. 6. Ankola landslide site location.

rainfall. This heavy rainfall likely caused the soil to become saturated and triggering the landslide. This tragic event led to the loss of nine lives, residents of Karnataka and Tamil Nadu and disrupted transportation by obstructing NH-66 with debris. The landslide also buried a truck along with its driver in the riverbed, highlighting the sudden and severe impact of the landslide.

3.1. Landslide characterization from site investigation

The landslide at Ankola was characterized by a detailed site investigation that captured critical geospatial and morphological data. The landslide lies approximately 35 m from the nearest road and 86 m from the river Gangavali. The landslide measured approximately 107 m in length and 93 m in width, with a depth of 15 m, covering an area of 7460 m^2. The estimated volume of displaced material was approximately 98000 m^3, which represents a significant mass movement. Additionally, the run-out distance extends to 180 m, emphasizing the landslide's mobility and the impact of the mass flow. Fig. 7a–e shows images of Ankola landslide site. The exposed bedrock in Fig. 7b showcases gneissic and granitic bedrock with noticeable weathered layers,

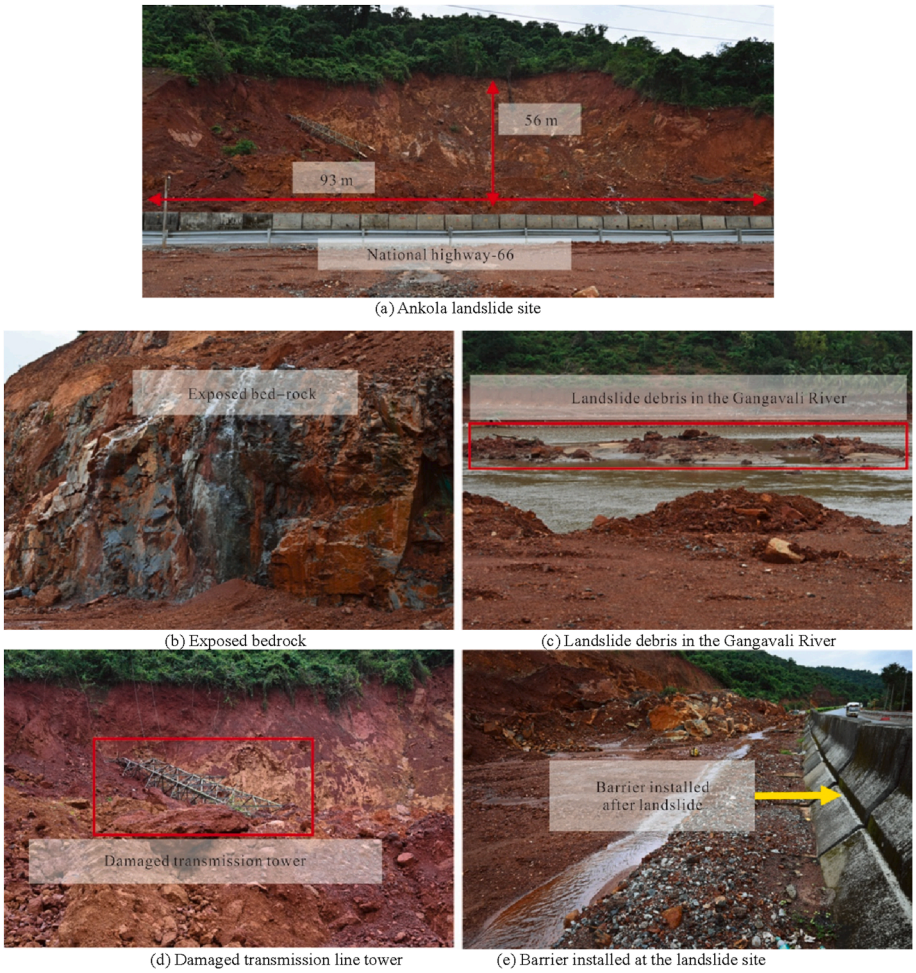

Fig. 7. Ankola landslide site images.

indicating weakened structural integrity, particularly under heavy rainfall conditions. The deposition of a substantial amount of landslide debris in the river shows the magnitude of the landslide event. A transmission tower was completely collapsed and buried in the landslide debris. As an immediate protective measure to the active NH-66, a barrier wall was installed along the roadside to prevent further landslide debris from reaching the highway.

3.2. Geotechnical characteristics

The geotechnical characterization of the landslide site provides valuable insights into the soil properties influencing slope stability. The particle size distribution curve of the soil collected from the landslide site is presented in Fig. 8. The soil properties evaluated in the laboratory is presented in Table 4. It reveals a composition of fine particles, with significant percentages in the silt and sand. The soil composition includes 8.24 % gravel, 49.62 % sand, 33.11 % silt, and 9.03 % clay, categorizing it as silty sand (SM) according to Indian standard soil classification systems. The soil has a specific gravity of 2.64 and a very low permeability rate of 6.55×10^{-8} m/s indicates limited water infiltration, potentially leading to pore pressure buildup during heavy rainfall. Additionally, the bedrock characteristics in the Western Ghats region play a significant role in slope stability. The bedrock in this region is primarily composed of gneissic and granitic formations with weathered layers at the surface. Studies have shown that these rocks are often fractured and weathered in the upper layers, which makes the slopes more susceptible to failure under rainfall conditions.

3.3. Rainfall history

The rainfall is considered the primary triggering factor of landslides in the Western Ghats [46]. Fig. 9a illustrates the annual monsoon rainfall recorded in the study area over the past 30 years, highlighting significant inter-annual variability. The data revealed that rainfall amounts have fluctuated notably, with some years experiencing extreme rainfall events surpassing 4000 mm, such as in 2003, 2011, and 2021, while other years exhibited considerably lower totals. These variations point to the unpredictable and intense nature of monsoon precipitation in the Western Ghats, which can have serious implications for landslide risk. High rainfall years are particularly concerning for slope stability, as prolonged and excessive rainfall can lead to soil saturation, increased pore water pressure, and subsequent slope failures. The variability observed over the decades suggests that there is a trend of irregularity in rainfall patterns. Understanding these trends is crucial for disaster preparedness and effective risk management in this landslide-prone region.

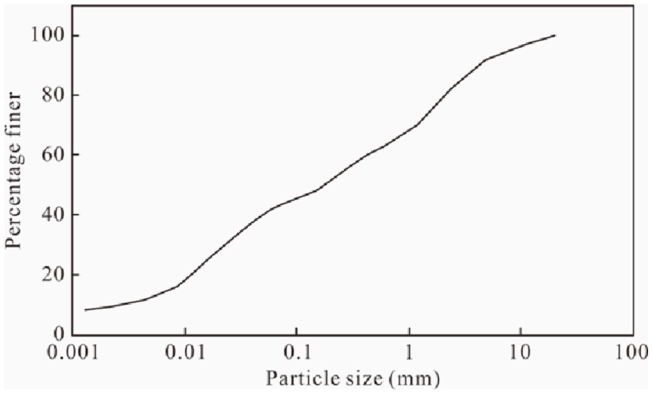

Fig. 8. Particle size distribution curve of soil sample.

Table 4
Soil properties.

Property	Value
Specific gravity	2.64
Gravel	8 %
Sand	50 %
Silt	33 %
Clay	9 %
Classification of soil	SM
Cohesion	44 kPa
Friction angle	31°
Permeability	6.55×10^{-8} m/s

Fig. 9b shows the maximum daily rainfall recorded during the monsoon season over the past 30 years in the study area. The data highlighted significant variability in extreme rainfall events, with certain years experiencing peak daily rainfall surpassing 250 mm, such as in 1995, 2003, and 2014. These high-intensity rainfall events are critical to understanding landslide risk, as sudden and extreme precipitation can lead to rapid soil saturation, increased water pressure, and immediate slope failures. The trend also suggests that the area is periodically subjected to rainfall events capable of triggering landslides, underscoring the importance of incorporating such data into landslide susceptibility modeling and early warning systems.

Fig. 9c illustrates daily and cumulative rainfall in July 2024, a critical month for understanding the conditions leading up to the Ankola landslide event on 16th July. The blue bars represent daily rainfall, and the red line indicates the cumulative rainfall. The data shows a marked increase in rainfall intensity between the 12th and 16th of July, with a pronounced spike on the 16th, where daily rainfall reached a peak of nearly 200 mm. This sudden surge, combined with the already high cumulative rainfall of over 1000 mm by mid-month, likely played a pivotal role in triggering the landslide.

3.4. Ankola landslide failure analysis

The geomorphological profile of the Ankola landslide slope was derived from a digital elevation model (DEM), sourced from sentinel satellite imagery. Fig. 10 represents the slope geometry, indicating a vertical rise of approximately 150 m across a horizontal distance of about 500 m. The gradient of the slope varies significantly, beginning nearly flat adjacent to National Highway 66 and increasing to a steep incline of up to 31° towards the midpoint of the slope. The stability of the slope was analysed using the Slide 2 module of the Rocscience software, which employs the limit equilibrium method to evaluate potential failure conditions. Specifically, the Spencer method was adopted due to its ability to comprehensively balance both force and moment equilibrium, providing a detailed assessment of slope stability [47]. The pore water pressure factor (R_u) factor was incorporated to simulate the impact of rainfall on slope stability. This parameter models showed the reduction in soil strength due to increased pore water pressure during rainfall events [48]. This approach allows for an accurate representation of landslide event induced by heavy rainfall. The R_u factor is defined as the ratio of pore water pressure to the total vertical stress exerted within the soil matrix [49]. Mathematically the R_u factor is expressed as Eq. (3).

$$R_u = \frac{u}{\sigma_v} \tag{3}$$

where u is the pore water pressure; and σ_v is the total vertical stress.

The analysis showcases how increasing pore water pressure, represented by the R_u factor, affects the factor of safety (FoS) of a slope. In Fig. 11a, the slope was analysed with R_u factor of 0.3, resulting in a factor of safety of 1.165. This value indicates that the slope maintains stability under these conditions. Conversely, Fig. 11b shows the slope with R_u factor increased to 0.5, where the FoS drops to 0.859. It represents an extensive reduction in stability of the slope, highlighting increased risk of failure.

Fig. 12 portrays relationship between the R_u and the factor of safety (FoS) for slope stability. It shows a linear decrease in stability of slope as

Fig. 9. Rainfall history of the Ankola region.

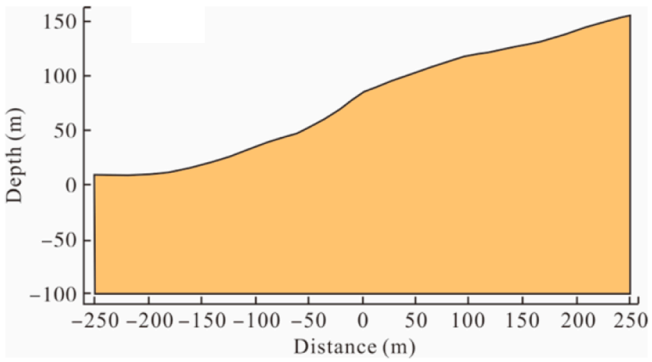

Fig. 10. Geometry of the Ankola landslide slope.

the R_u factor increases from 0 to 1. This plot points out the critical thresholds where the FoS approaches and then falls below 1, a point indicating potential slope failure. From the plot, it is obvious that the FoS begins at an optimal level of approximately 1.6 when the R_u factor is zero, indicating that the slope is entirely stable under dry conditions. As the R_u factor increases, reflecting increased pore water pressures due to rainfall, the FoS correspondingly decreases. The plot shows a critical transition at the R_u of about 0.4, where the FoS descends below the stability threshold of 1.0. Beyond this point, the risk of slope failure becomes pronounced. This linear relationship is crucial for developing rainfall threshold for this region. For instance, areas prone to high rainfall can see rapid increases in R_u values, pushing the FoS below the safety threshold and thereby raising the likelihood of landslide. The R_u vs. FoS plot can be used to establish specific rainfall thresholds, that once exceeded, would likely increase the R_u factor to a level that critically reduces the FoS. By doing so, it is possible to implement preventive measures such as evacuation orders or the stabilization of slopes before anticipated heavy rains.

In addition to rainfall-induced instability, anthropogenic factors likely contributed to the slope failure at Ankola. Unregulated slope

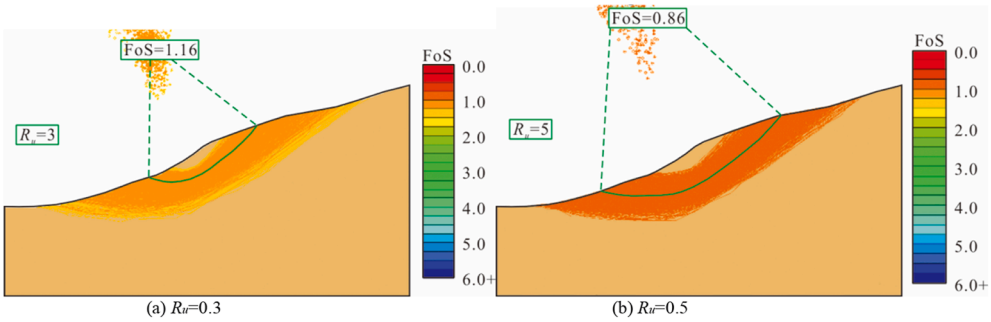

Fig. 11. Factor of safety of the slope.

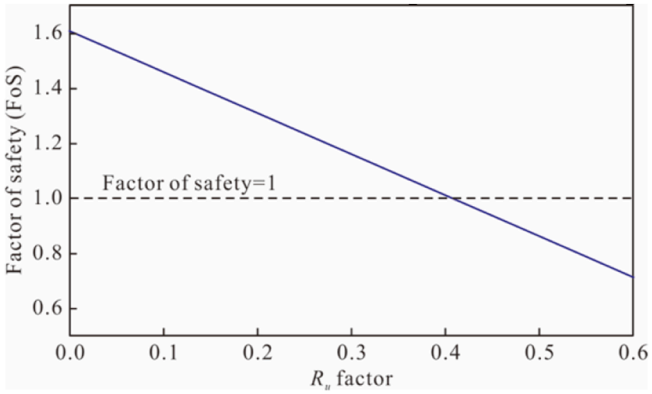

Fig. 12. Variation of factor of safety with R_u factor.

modification, landcover change, and unscientific construction activities near the toe of the slope have altered the natural drainage patterns and reduced the shear strength of the soil mass. The proximity of infrastructure development along National Highway 66, could have introduced additional loading and vibrations, further exacerbating the susceptibility of the slope to failure during intense rainfall events.

4. Conclusions

The landslide susceptibility in the Western Ghats of Karnataka was conducted using a hybrid approach by leveraging historical landslide data and diverse geospatial datasets of causative factors. Further a case study of the 2024 Ankola landslide was incorporated to validate the susceptibility model. Following conclusions were made based on the analysis of susceptibility model and Ankola landslide site.

(1) The study underscores that 60.7 % of the Western Ghats region in Karnataka is susceptible to landslides. Among the susceptible area, 30 % is in the Uttara Kannada district followed by Shivamogga (17.18 %), Chikkamagaluru (17 %), Kodagu (13.88 %), Dakshina Kannada (9.63 %), Hassan (8.26 %), and Udupi (4 %). This highlights the need for enhanced monitoring and preventive strategies in these highly susceptible area areas.
(2) The hybrid methodology successfully assessed landslide susceptibility in the Western Ghats of Karnataka, achieving an AUC value of 0.902. This high AUC value confirms that the model effectively distinguishes between landslide susceptible and non-susceptible zones.
(3) Rainfall, slope, and soil type are the primary factors influencing landslide susceptibility in the study area. Particularly, the regions with more than 3000 mm annual rainfall, consisting clayey loam soil, and slope gradient more than 28°, are very much likely to have landslides.
(4) The Ankola landslide site has slope gradient up to 31° and receives more than 3000 mm rainfall annually. With the presence of other causative factors like proximity to road and river, the landslide event validates the landslide susceptibility map developed by the hybrid method.
(5) The R_u factor of 0.4 has emerged as a critical threshold for slope stability in the study area, indicating the point at which slope failure becomes likely under rainfall conditions. This threshold can be utilized in early warning systems to predict and mitigate landslide risks in advance.
(6) Anthropogenic activities such as unregulated slope cutting, landcover change, and unscientific construction activities near the highway likely contributed to the Ankola landslide on July 16, 2024.

The study provides a robust framework for landslide susceptibility assessment in the Western Ghats. However, the study has certain limitations. One limitation is that climate change impacts on landslide susceptibility were not considered. Future research may incorporate downscaled climate model projections to capture long-term variations in rainfall intensity and frequency. This would improve the prediction of landslide susceptibility under changing climate conditions. In addition, the validation of event-based hydrological thresholds represents a potential research direction. The R_u value can be assessed using broader datasets and regional models to strengthen its applicability in early warning systems.

CRediT authorship contribution statement

Malay Pramanik: Writing – original draft, Visualization, Methodology, Investigation, Formal analysis, Data curation, Conceptualization. **Amarnath Hegde:** Writing – review & editing, Supervision, Resources, Methodology, Conceptualization.

Declaration of competing interest

The authors declare that they have no known competing financial interests or personal relationships that could have appeared to influence the work reported in this paper.

Acknowledgements

No funding was received for conducting this study.

References

[1] M.J. Froude, D.N. Petley, Global fatal landslide occurrence from 2004 to 2016, Nat. Hazards Earth Syst. Sci. 18 (2018) 2161–2181.
[2] M. Karpouza, H.D. Skilodimou, G. Kaviris, A. Zymvragakis, A. Antonarakou, G. D. Bathrellos, Escape routes and safe points in natural hazards. A case study for soil, Eng. Geol. 340 (2024) 107683.
[3] L. Shano, T.K. Raghuvanshi, M. Meten, Landslide susceptibility evaluation and hazard zonation techniques – a review, Geoenvironmental Disasters 7 (2020) 18.

[4] H.R. Pourghasemi, B. Pradhan, C. Gokceoglu, Application of fuzzy logic and analytical hierarchy process (AHP) to landslide susceptibility mapping at haraz watershed, Iran, Nat. Hazards 63 (2012) 965–996.
[5] A.M. Youssef, B.A. El Haddad, H.D. Skilodimou, G.D. Bathrellos, F. Golkar, H. R. Pourghasemi, Landslide susceptibility, ensemble machine learning, and accuracy methods in the southern sinai peninsula, Egypt: assessment and mapping, Nat. Hazards 120 (2024) 14227–14258.
[6] X. Wang, F. Huang, X. Fan, H. Shahabi, A. Shirzadi, H. Bian, X. Ma, X. Lei, W. Chen, Landslide susceptibility modeling based on remote sensing data and data mining techniques, Environ. Earth Sci. 81 (2022) 50.
[7] P. Reichenbach, M. Rossi, B.D. Malamud, M. Mihir, F. Guzzetti, A review of statistically-based landslide susceptibility models, Earth Sci. Rev. 180 (2018) 60–91.
[8] M. Aniya, Landslide-susceptibility mapping in amahata river basin, Ann. Assoc. Am. Geogr. 75 (1985) 102–114.
[9] C.J. van Westen, T.W.J. van Asch, R. Soeters, Landslide hazard and risk zonation - why is it still so difficult? Bull. Eng. Geol. Environ. 65 (2) (2006) 167–184.
[10] N.R. Regmi, J.R. Giardino, J.D. Vitek, Modeling susceptibility to landslides using the weight of evidence approach: western Colorado, USA, Geomorphology 115 (2010) 172–187.
[11] L. Feng, M. Zhang, Y. Mao, H. Liu, C. Yang, Y. Dong, Y.A. Nanehkaran, Convolutional neural network-based deep learning for landslide susceptibility mapping in the bakhtegan watershed, Sci. Rep. 15 (2025) 13250.
[12] S.K. Roy, S. Dey, J. Das, B. Hossen, S. Das, M.M. Hasan, P. Mojumder, Utilising machine learning approaches for enhanced landslide susceptibility mapping in Sikkim, India, Geol. J. 60 (5) (2025) 1150–1169.
[13] G. Agboola, L.H. Beni, T. Elbayoumi, G. Thompson, Optimizing landslide susceptibility mapping using machine learning and geospatial techniques, Ecol. Inform. 81 (2024) 102583.
[14] A. Arabameri, S. Chandra Pal, F. Rezaie, R. Chakrabortty, A. Saha, T. Blaschke, M. Di Napoli, O. Ghorbanzadeh, P.T. Thi Ngo, Decision tree based ensemble machine learning approaches for landslide susceptibility mapping, Geocarto Int. 37 (2022) 4594–4627.
[15] M. Azarafza, M. Azarafza, H. Akgün, P.M. Atkinson, R. Derakhshani, Deep learning-based landslide susceptibility mapping, Sci. Rep. 11 (1) (2021) 24112.
[16] A. Merghadi, A.P. Yunus, J. Dou, J. Whiteley, B. ThaiPham, D.T. Bui, R. Avtar, B. Abderrahmane, Machine learning methods for landslide susceptibility studies: a comparative overview of algorithm performance, Earth Sci. Rev. 207 (2020) 103225.
[17] J.N. Goetz, A. Brenning, H. Petschko, P. Leopold, Evaluating machine learning and statistical prediction techniques for landslide susceptibility modeling, Comput. Geosci. 81 (2015) 1–11.
[18] J. Barman, B. Biswas, K.S. Rao, A hybrid integration of analytical hierarchy process (AHP) and the multiobjective optimization on the basis of ratio analysis (MOORA) for landslide susceptibility zonation of aizawl, India, Nat. Hazards 120 (2024) 8571–8596.
[19] H.A.H. Al-Najjar, B. Pradhan, X. He, D. Sheng, A. Alamri, S. Gite, H.J. Park, Integrating physical and machine learning models for enhanced landslide prediction in data-scarce environments, Earth Systems and Environment 9 (4) (2025) 3179–3206.
[20] A. Singh, S. Pal, D.P. Kanungo, An integrated approach for landslide susceptibility–vulnerability–risk assessment of building infrastructures in hilly regions of India, Environ. Dev. Sustain. 23 (2021) 5058–5095.
[21] R.A. Mir, Z. Habib, A. Kumar, N.A. Bhat, Landslide susceptibility mapping and risk assessment using total estimated susceptibility values along NH44 in Jammu and Kashmir, Western himalaya, Nat. Hazards 120 (2024) 4257–4296.
[22] S.N. Chellamuthu, G.P. Ganapathy, Quantifying the impact of changing rainfall patterns on landslide frequency and intensity in the nilgiris district of Western ghats, India, Prog. Disaster Sci. 23 (2024) 100351.
[23] S. Kolathayar, V. Menon, P. Kundu, Landslides and debris flow triggered by the July 2024 extreme rainstorm in the chooralmala watershed in wayanad, India, Landslides (2024) 967–974.
[24] National Landslide Risk Mitigation Programme, NLRMP) Phase-1. https://ndma.gov.in/node/511, 2025. (Accessed 13 August 2025).
[25] K.S. Sajinkumar, S. Anbazhagan, Geomorphic appraisal of landslides on the windward slope of Western ghats, southern India, Nat. Hazards 75 (2015) 953–973.
[26] H. Vijith, K.N. Krishnakumar, G.S. Pradeep, M.V. Ninu Krishnan, G. Madhu, Shallow landslide initiation susceptibility mapping by GIS-based weights-of-evidence analysis of multi-class spatial data-sets: a case study from the natural sloping terrain of Western ghats, India, Georisk 8 (2014) 48–62.
[27] B. Feby, A.L. Achu, K. Jimnisha, V.A. Ayisha, R. Reghunath, Landslide susceptibility modelling using integrated evidential belief function based logistic regression method: a study from southern Western ghats, India, Remote Sens. Appl. 20 (2020) 100411.
[28] S. Bera, B. Guru, V. Ramesh, Evaluation of landslide susceptibility models: a comparative study on the part of Western Ghat region, India, Remote Sens. Appl. 13 (2019) 39–52.
[29] S.K. Wadhawan, B. Singh, M.V. Ramesh, Causative factors of landslides 2019: case study in malappuram and wayanad districts of Kerala, India, Landslides 17 (2020) 2689–2697.
[30] X. Gao, Development laws of geological hazards along urban highway in southwest China and countermeasures for prevention and control, Geohazard Mechanics 2 (2024) 13–20.
[31] D.P. Kanungo, M.K. Arora, S. Sarkar, R.P. Gupta, A fuzzy set based approach for integration of thematic maps for landslide susceptibility zonation, Georisk 3 (2009) 30–43.
[32] M. Ahmed, G. Titti, S. Trevisani, L. Borgatti, M. Francioni, Is higher resolution always better? A comparison of open-access DEMs for optimized slope unit delineation and regional landslide prediction, Nat. Hazards Earth Syst. Sci. 25 (2025) 2519–2539.
[33] K.T. Chang, A. Merghadi, A.P. Yunus, B.T. Pham, J. Dou, Evaluating scale effects of topographic variables in landslide susceptibility models using GIS-Based machine learning techniques, Sci. Rep. 9 (2019) 12296.
[34] G.D. Bathrellos, I.K. Koukouvelas, H.D. Skilodimou, K.G. Nikolakopoulos, A. L. Vgenopoulos, Landslide causative factors evaluation using GIS in the tectonically active glafkos river area, northwestern Peloponnese, Greece, Geomorphology 461 (2024) 109285.
[35] M.T. Abraham, N. Satyam, P. Jain, B. Pradhan, A. Alamri, Effect of spatial resolution and data splitting on landslide susceptibility mapping using different machine learning algorithms, Geomat. Nat. Hazards Risk 12 (2021) 3381–3408.
[36] M.I. Sameen, B. Pradhan, D.T. Bui, A.M. Alamri, Systematic sample subdividing strategy for training landslide susceptibility models, Catena 187 (2020) 104358.
[37] U. Ozturk, M. Pittore, R. Behling, S. Roessner, L. Andreani, O. Korup, How robust are landslide susceptibility estimates? Landslides 18 (2021) 681–695.
[38] S. Mandal, K. Mandal, Bivariate statistical index for landslide susceptibility mapping in the rorachu river basin of eastern Sikkim himalaya, India, Spatial Information Research 26 (2018) 59–75.
[39] A. Tyagi, N. Gupta, R.K. Tiwari, N. James, S.R. Chavan, Determining the impact of anthropogenic activities and climate change on landslide susceptibility for the himalayan region, Nat. Hazards 121 (2025) 5239–5265.
[40] I. Das, A. Stein, N. Kerle, V.K. Dadhwal, Landslide susceptibility mapping along road corridors in the Indian himalayas using Bayesian logistic regression models, Geomorphology 179 (2012) 116–125.
[41] A. Rahaman, A. Dondapati, S. Gupta, R. Raj, Leveraging artificial neural networks for robust landslide susceptibility mapping: a geospatial modeling approach in the ecologically sensitive nilgiri district, Tamil Nadu, Geohazard Mechanics 2 (2024) 258–269.
[42] T.L. Saaty, Decision making with the analytic hierarchy process, Int. J. Services Sciences 1 (2008) 83–98.
[43] A. Yalcin, S. Reis, A.C. Aydinoglu, T. Yomralioglu, A GIS-based comparative study of frequency ratio, analytical hierarchy process, bivariate statistics and logistics regression methods for landslide susceptibility mapping in Trabzon, NE Turkey, Catena 85 (2011) 274–287.
[44] D. Gaikwad, A. Tyagi, R.K. Tiwari, Hybrid FR-AHP approach for GLOF hazard assessment in the himalayan region, Remote Sens. Appl. (2025) 101437.
[45] K.K. Fatah, Y.T. Mustafa, I.O. Hassan, Geoinformatics-based frequency ratio, analytic hierarchy process and hybrid models for landslide susceptibility zonation in Kurdistan region, northern Iraq, Environ. Dev. Sustain. 26 (2024) 6977–7014.
[46] D. Choudhury, T. Das, V.D. Rao, Case studies and numerical investigation of landslide triggering mechanisms in Western ghats, Kerala, India, Indian Geotech. J. 54 (2024) 96–108.
[47] J.M. Duncan, S.G. Wright, The accuracy of equilibrium methods of slope stability analysis, Eng. Geol. 16 (1980) 5–17.
[48] S. Vadivel, C.S. Sennimalai, Failure mechanism of long-runout landslide triggered by heavy rainfall in achanakkal, nilgiris, India, J. Geotech. Geoenviron. Eng. 145 (2019) 04019047.
[49] P.R. Vaughan, H.J. Walbancke, Pore pressure changes and the delayed failure slopes in overconsolidated clay, Geotechnique 23 (1973) 531–539.